



Chronic Fluoxetine Induces Activity Changes in Recovery From Poststroke Anxiety, Depression, and Cognitive Impairment

Faranak Vahid-Ansari¹ · Paul R. Albert¹

Published online: 4 December 2017
© The American Society for Experimental NeuroTherapeutics, Inc. 2017

Abstract

Poststroke depression (PSD) is a common outcome of stroke that limits recovery and is only partially responsive to chronic antidepressant treatment. In order to elucidate changes in the cortical-limbic circuitry associated with PSD and its treatment, we examined a novel mouse model of persistent PSD. Focal endothelin-1-induced ischemia of the left medial prefrontal cortex (mPFC) in male C57BL6 mice resulted in a chronic anxiety and depression phenotype. Here, we show severe cognitive impairment in spatial learning and memory in the stroke mice. The behavioral and cognitive phenotypes were reversed by chronic (4-week) treatment with fluoxetine, alone or with voluntary exercise (free-running wheel), but not by exercise alone. To assess chronic cellular activation, FosB⁺ cells were co-labeled for markers of glutamate/pyramidal (VGluT1-3/CaMKII α), γ -aminobutyric acid (GAD67), and serotonin (TPH). At 6 weeks poststroke *versus* sham (or 4 days poststroke), left mPFC stroke induced widespread FosB activation, more on the right (contralesional) than on the left side. Stroke activated glutamate cells of the mPFC, nucleus accumbens, amygdala, hippocampus, and raphe serotonin neurons. Chronic fluoxetine balanced bilateral neuronal activity, reducing total FosB and FosB/CamKII⁺ cells (mPFC, nucleus accumbens), and unlike exercise, increasing FosB/GAD67⁺ cells (septum, amygdala) or both (hippocampus, raphe). In summary, chronic antidepressant but not exercise mediates recovery in this unilateral ischemic PSD model that is associated with region-specific reversal of stroke-induced pyramidal cell hyperactivity and increase in γ -aminobutyric acid activity. Targeted brain stimulation to restore brain activity could provide a rational approach for treating clinical PSD.

Keywords Poststroke depression · Antidepressant · Exercise · Serotonin · Cognitive function · Prefrontal cortex

Introduction

Poststroke depression (PSD) is a common consequence of stroke that occurs within 3 months of a stroke in 30% of patients [1, 2]. Patients that suffer PSD often have anxiety, cognitive impairment [3, 4], and increased overall mortality within 10 years [5, 6]. PSD is typically treated with selective serotonin reuptake inhibitors (SSRIs) like fluoxetine (FLX), but SSRIs require chronic treatment (3–4 weeks) to increase serotonin (5-HT) and improve depressive behavior [7]. In addition, SSRI treatment may enhance cognitive and motor recovery [8–11]. However, although 50% of depressed patients respond initially to SSRIs, remission is seen in only 30%.

Furthermore, SSRI treatment is associated with an increased risk of severe hemorrhagic stroke and mortality [5, 12]. Hence, improved approaches to more effectively treat PSD are needed to enhance stroke recovery.

Patients with PSD often undergo concurrent rehabilitation therapy involving exercise that may also have an antidepressant effect, but the clinical data remain unclear [13]. In pre-clinical rodent models, free wheel-running exercise has antidepressant and cognitive enhancing effects, including increasing hippocampal brain-derived neurotrophic factor, neurogenesis, and synaptic plasticity [14, 15]. Combining SSRI and exercise may have enhanced antidepressant activity and may improve cognitive and motor recovery [8–11]. Chronic exercise might augment SSRI action through activation of the 5-HT system [16, 17], but it remains unclear whether these treatments interact to enhance recovery from PSD [18].

In order to address the actions of SSRIs or exercise in recovery from PSD, we developed a highly specific mouse

✉ Paul R. Albert
palbert@uottawa.ca

¹ Ottawa Hospital Research Institute (Neuroscience), UOttawa Brain and Mind Research Institute, Ottawa, ON K1H 8M5, Canada

model of chronic PSD [19]. The current middle cerebral artery occlusion (MCAO) rodent models of PSD have several limitations [20]. Depression-like behavior is observed in these models, but only after stressors that alone induce depression, confounding the poststroke phenotype [20]. Furthermore, MCAO results in large and variable lesions, with sensorimotor impairments that may confound the evaluation of behavioral phenotypes. To refine the PSD model, we used unilateral microinjection of the vasoconstrictor endothelin 1 (ET-1) into the left medial prefrontal cortex (mPFC) to produce a small ischemic lesion that resulted in a robust PSD phenotype without sensorimotor impairment [19]. The left mPFC was targeted based on evidence that ischemic lesions affecting the left mPFC or its projections are associated with depression-like behavior following stroke [20]. While anterior cerebral artery strokes that affect the mPFC are rare, our model mimics more common disruption to the mPFC–raphe circuitry implicated in anxiety–depression phenotypes [21–23].

Our stroke mice display robust anxiety and depression phenotypes at 1 week poststroke, persisting for at least 6 weeks poststroke with no spontaneous improvement, providing a useful model to study chronic recovery [19]. Here, we identify a severe cognitive impairment in this model and address whether chronic treatment with FLX and/or voluntary exercise results in recovery from poststroke behavioral and cognitive impairments. We have also examined brain-wide changes in FosB expression as a marker of chronic activation in specific cell types following PSD and treatment [24]. Our results indicate that recovery is associated with a partial reversal of stroke-induced changes in FosB⁺ cells at specific nodes of the anxiety–depression circuitry. Our results indicate that chronic SSRI, alone or with exercise, rebalances activation of the PFC–raphe–limbic circuitry to mediate recovery from PSD.

Methods

Animals

One hundred and four 11-week-old male C57/BL6 mice (Charles River Laboratories, Montreal, QC, Canada) weighing 25 to 28 g at the time of surgery were used in this study. Mice were single-housed in standard Plexiglass cages on a 12/12 h light/dark cycle with *ad libitum* access to food and water. Animals were allowed to acclimate to the housing facility for 2 weeks prior to surgery. Mice were behaviorally tested in different cohorts of 4 to 32 mice after surgery and/or chronic treatment, and some were perfused for postmortem histology (Table 1). Cohort 1 of PSD mice ($n = 4$) was used 4 days poststroke for histology. Another group of mice ($n = 20$) was equally divided into sham control and stroke and used 6-weeks poststroke for histology studies.

For the combined treatment study (cohort 2), a group of mice ($n = 24$) was randomly assigned to either sham control ($n = 12$) surgery and [subjected to fixed wheels and sucrose 1% (vehicle)] or a stroke group ($n = 12$) subjected to voluntary exercise and 18 mg/kg/day FLX hydrochloride (Cedarlane, Hornby, ON, Canada), starting at 1 week postsurgery. Voluntary exercise constituted free access to running wheels in the home cages and the number of wheel rotations/day was monitored. Next, 2 separate cohorts (cohorts 3 and 4) were used for behavioral assays and histology after chronic monotherapy (for 3–4 weeks). These cohorts of mice ($n = 32$ /cohort; 8/group) were randomly divided into 3 stroke groups and 1 sham control group. At 1-week postsurgery, the sham and PSD mice received sucrose 1% and fixed wheels (sham or vehicle groups, respectively), sucrose 1% and running wheels (RW) or FLX (80 mg/l in 1% sucrose, *ad libitum* to reach 18 mg/kg/day, p.o. [25]) and fixed wheels (FW). FLX was prepared in opaque bottles to protect it from light and liquid consumption was measured every day for the first week; every 2 days in the second week; and thereafter every 3 days to the end of treatment. For vehicle and FLX groups, the mean \pm SD liquid consumption was 7.1 ± 0.4 and 6.1 ± 0.7 ml/day, respectively; and weight was 26.5 ± 0.3 and 27.3 ± 0.6 g at sacrifice. The automated wheel revolutions were assessed every 2 days and for the PSD/RW group the total distance was consistent between mice and was $72,660 \pm 6280$ m/mouse (mean \pm SEM; $n = 8$) for 3 weeks. For the combination treatment group, liquid consumption was 5.8 ± 0.7 ml versus sham ctrl 6.1 ± 0.4 ml; rotations were 68340 ± 2070 ; and body weight was 25.8 ± 0.7 g versus sham ctrl 27.1 ± 0.4 g. The University of Ottawa Animal Care Committee approved all experimental procedures in accordance with guidelines established by the Canadian Council of Animal Care.

ET-1-Induced PSD Model

PSD was induced as described previously [19] by consecutive microinjections of 1 μ l ET-1 (2 μ g/ μ l = 800 pmol/ μ l) at 2 sites [19]: first, anterior–posterior, 2.0; medial–lateral, +0.5; dorsoventral, –2.4; second, anterior–posterior 1.5; medial–lateral +0.5; dorsoventral –2.6. Sham control mice underwent the same procedure except that the ET-1 was replaced with vehicle (sterile water). The mice were placed in a 37°C incubator to maintain body temperature until they regained mobility and were treated with 0.1 ml 2% transdermal bupivacaine (Chiron, Guelph, ON, Canada) as a topical anesthetic and 2 injections of buprenorphine (0.03 mg/kg, s.c.; Reckitt Benckiser Pharmaceuticals, Richmond, VA, USA) for pain management for 3 h postsurgery. For all cohorts, at 4 days poststroke, brains were visualized using a 7-T GE/Agilent magnetic resonance imager (University of Ottawa Preclinical Imaging Core Facility) in living animals, and the lesion area quantified using ImageJ as previously described [19].

Table 1 Mouse cohorts for behavioral testing

Cohort	<i>n</i>	MRI 4 days	Behavior (7 days)	Treatment (3–4 weeks)	Behavior (4–6 weeks)	IF (6 weeks)
1	4	+	–	–	–	+
2	20	+	EPM	–	EPM	+
3	24	+	EPM	FLX+Exc	EPM, OF, FST, TS, NSF	+
4	32	+	EPM	FLX/Exc/veh	EPM, OF, FST, TS, NSF, MWM	+
5	24	+	EPM	FLX/Exc/veh	EPM, OF, FST, TS, NSF	+

A summary of mouse cohorts used for behavioral studies showing: the number of mice; magnetic resonance imaging (MRI) at 4 days poststroke; behavior tests done at 7 days poststroke or after treatment, 4–6 weeks poststroke; treatment for 3–4 weeks starting 1 week poststroke; and immunofluorescence (IF) following behavioral studies

EPM = elevated plus maze; OF = open field test; FST = forced swim test; TS = tail suspension test; NSF = novelty suppressed feeding test; MWM = Morris water maze; FLX = fluoxetine; Exc = exercise; Veh = vehicle

Immunofluorescence

For immunofluorescence studies, mice were euthanized by Euthanyl (149.5 mg/kg i.p.; Bimeda-MTC Health, Cambridge, ON, Canada) and perfused by cardiac puncture with chilled phosphate-buffered saline (PBS) and then with 4% paraformaldehyde for fixation. Whole brains were isolated, cryo-protected overnight in 20% sucrose, and frozen at –80°C. Coronal brain slices (25- μ m thickness) were prepared using the coordinates summarized in Table 2. Slices were

Table 2 Coordinates relative to Bregma of regions assessed by immunofluorescence

Brain region	Distance from Bregma
mPFC	1.7
CGctx	1.7
PI	1.7
NAc	1.1
LSN	0.5
HBL	–2.07
Hippocampus	–1.7
CA1	–1.7
CA2	–1.7
CA3	–1.7
DG	–1.7
Amygdala	–2.06
DR	–4.36 to –4.72
DDR	–4.36 to –4.72
VDR	–4.36 to –4.72
LDR	–4.36 to –4.72
VLDR	–4.36 to –4.72

mPFC = medial prefrontal cortex; CGctx = cingulate cortex; PI = preinfra/limbic; NAc = nucleus accumbens; LSN = lateral septal nucleus; HBL = lateral habenular nucleus; DG = dentate gyrus; DR = dorsal raphe; DDR = dorsal DR; VDR = ventral DR; LDR = lateral DR; VLDR = ventrolateral DR

thaw-mounted on Superfrost slides (Thermo-Fisher, Waltham, MA, USA) and kept at –80°C. The sections were washed 3 times in PBS, blocked for 1 h in PBS with 1% bovine serum albumin, 10% donkey serum (NDS), 0.1% Triton X-100, followed by 24 h incubation (unless indicated otherwise) at 22°C with the primary antibodies listed in Table 3. The sections were then washed 3 times in PBS and incubated for 1 h in secondary antibodies at 22°C in blocking solution (see Table 3). Images were acquired with Axiovision imaging software on a Zeiss Axio Observer D1 microscope under 10 \times and 20 \times magnification ($n = 4$ /group). The number of FosB/4',6-diamidino-2-phenylindole-(DAPI)positive cells was counted on images taken under 20 \times magnification of 20- μ m slices at coordinates indicated in Table 2 from 4 mice. A coding system was used so that the counter was blind to the treatment. Nuclear FosB⁺ staining marked by 4',6-diamidino-2-phenylindole surrounded with GAD67 or CaMKII α /VGluT3 was counted as FosB/GAD67⁺ or FosB-CaMKII α /VGluT3⁺ cells. FosB⁺ cells were quantified per area/section and the mean values were then averaged ($n = 4$). For DR, FosB/tryptophan hydroxylase (TPH)⁺, FosB/VGluT3⁺, and FosB/GAD67⁺ cells were quantified at 4 different levels of middle dorsal raphe (DR)/mouse and averaged ($n = 4$).

Behavioral Assays

Behavioral tests were performed following either at 1 week postsurgery or following 3 weeks of treatment (4 weeks poststroke). Mice were housed in 12h/12h light/dark conditions (lights on at 8:00 AM) and tests were performed beginning at 10:00 AM, after at least 1 h of habituation to the testing room. Testing was performed under white-light illumination or red light for the forced swim test (FST). For all cohorts, elevated plus maze (EPM) was done 1 week postsurgery (pretreatment) to verify the poststroke behavioral phenotype. Then, chronic treatment was begun and the mice were kept under

Table 3 Primary and secondary antibodies for immunofluorescence staining

	Host	Concentration	Company	Catalog number
Primary antibody				
CaMKII	R	1:100	Santa Cruz*	sc-9035
FosB	M	1:500	Abcam [†]	11959
FosB	R	1:500	Santa Cruz*	sc-48
GAD67	M	1:500	Millipore [‡]	135406
TPH	Sh	1:100	Millipore [‡]	ab1541
VGluT3	GP	1:100	Millipore [‡]	ab542ZI
Secondary antibody				
D/GP Cy5	–	1:250	Jackson Laboratory [§]	706-175-148
D/M Cy3	–	1:250	Jackson Laboratory [§]	715-163-160
D/R 488	–	1:1000	Life Technologies [¶]	A-21206
D/Sh Cy3	–	1:200	Jackson Laboratory [§]	713-165-003
G/GP 594	–	1:200	Life Technologies [¶]	A-11076
G/M Cy5	–	1:800	Abcam [†]	ab6563
G/R 594	–	1:200	Life Technologies [¶]	A-11037

Sections from different forebrain and midbrain regions ($n = 4$) were stained with different antibodies as listed in Table 2. The host to primary antibodies: D = donkey; G = goat; GP = guinea pig; M = mouse; R = rabbit; Sh = sheep. The host to secondary antibodies: D/GP = donkey antiguinea pig; D/M = donkey antimouse; D/R = donkey antirabbit; D/Sh = donkey antisheep; G/GP = goat antiguinea pig; G/M = goat antimouse; G/R = goat antirabbit. Label: Alexa 488, 594, Cy3 or Cy5

*Santa Cruz, CA, USA

[†] Cambridge, UK

[‡] Burlington, MA, USA

[§] Bar Harbor, ME, USA

[¶] Carlsbad, CA, USA

treatment until the last test day and perfused. At 3 weeks posttreatment behavioral tests were done in the following order: open field (OF), FST, tail suspension (TS), novelty-suppressed feeding (NSF), and a second EPM test, according to the timeline (Fig. 1). Throughout the testing and behavioral analyses, a coding system was used so that the experimenters were blind to the treatment groups.

EPM

Mice were placed in the center of an EPM (20 cm high, ~6 cm wide, and ~75 cm long; Noldus, Wageningen, the Netherlands) with the head toward the closed arm and allowed to explore the maze for 10 min, videotaped, and the time spent in closed and open arms analyzed (Ethovision 10; Noldus).

OF Test

Mice were placed in a corner of the arena (45 cm long × 45 cm high) for 10 min at light levels of 300 lux, videotaped, and the time spent in the center (24 × 15 cm) and corners (squares with 10-cm sides) analyzed (Ethovision 10; Noldus).

FST

Each mouse was placed into clear plastic cylinder (22 cm diameter × 37 cm deep) filled with 4 l water (24°C), videotaped for 6 min under red lighting, and the duration of immobility time quantified using video-tracking software from Med Associates (Ethovision XT; Noldus).

TS Test

The tail of the mouse was taped to a horizontal bar in a TS box (Med Associates) for 6 min. Immobility duration was measured using an automated detection device (ENV-505TS Load-Cell Amplifier; Med 28 Associates, Fairfax, VT, USA) and quantified using Ethovision XT software. The lower threshold (3) was set and the force recorded below the threshold was considered immobility.

NSF Test

Mice deprived of food for 16 h were individually placed in an arena (45 cm long × 45 cm high; 100 lux) with a food pellet placed in the center. The latency for the mice to begin eating food was recorded manually and immediately after mice

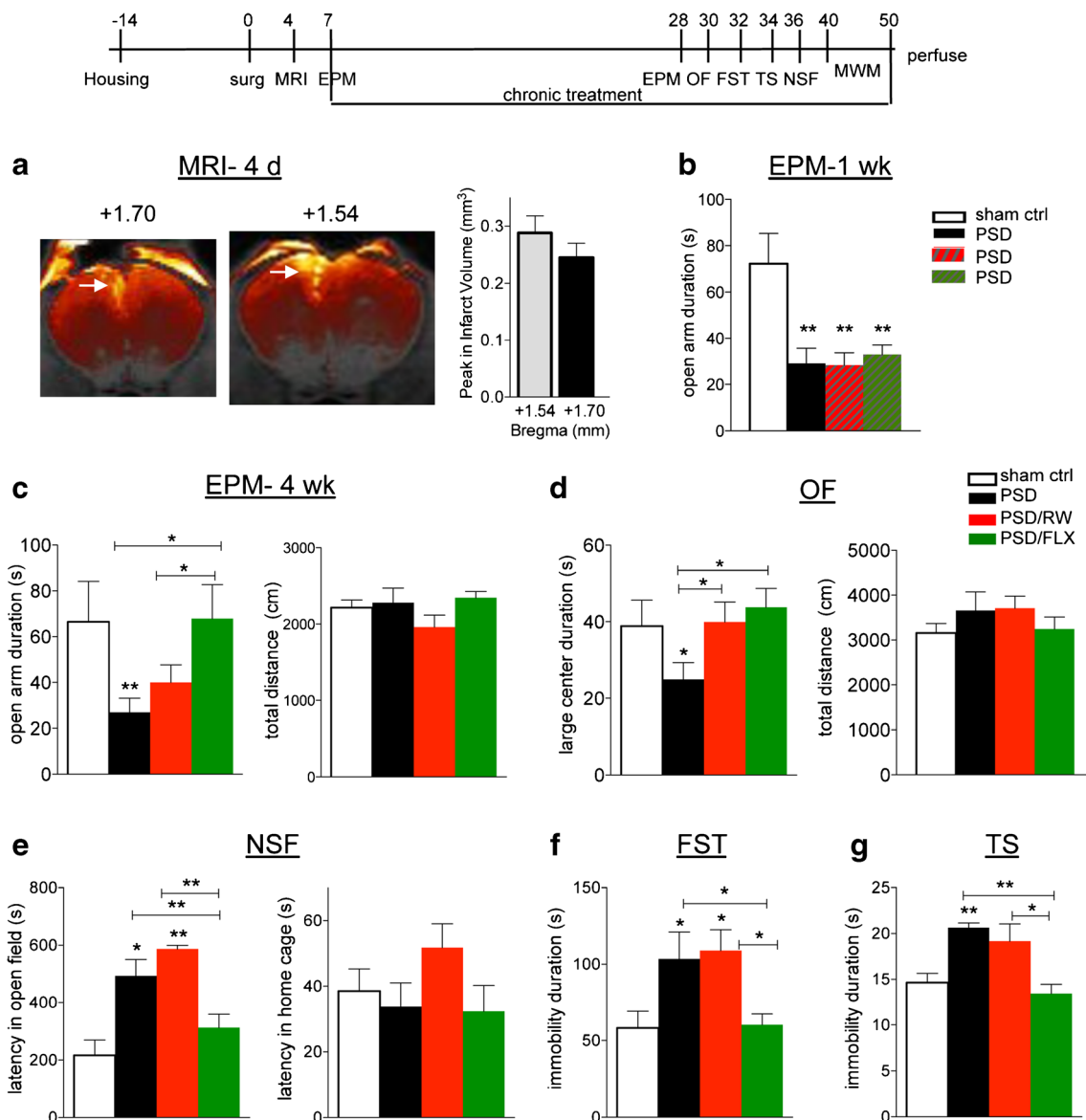


Fig. 1 Chronic fluoxetine (FLX), but not exercise, reverses behavioral phenotype in mice with poststroke depression (PSD). Timeline: mice were individually housed 14 days prior to surgery (Housing), microinjected with vehicle (sham ctrl) or endothelin 1 (ET-1; PSD) in the left medial prefrontal cortex (mPFC; surg, day 0); at 4 days poststroke, lesions were verified by magnetic resonance imaging (MRI), and at 7 days anxiety phenotype verified using elevated plus maze (EPM; 1 week); from 7 days onwards treatment was with FLX (PSD/FLX) or free running wheel (PSD/RW), with fixed wheel and vehicle as control (for PSD and sham ctrl) and compared with Sham-ctrl. Behavioral assays [EPM 4 weeks; open field (OF); forced swim test (FST); tail suspension (TS) test; novelty suppressed feeding test (NSF)] were done from days 28 to 40 followed by the Morris water maze (MWM; see Fig. 2) and perfusion (perfuse). (A) ET-1 lesion site visualized *in vivo* by MRI. Shown is a representative 7-Tesla MRI image done in an anaesthetized, living mouse at 4 days poststroke showing a 300- μ m MRI section in which the lesion site is visualized and limited to the left mPFC [left (L); right (R)]. Infarct volumes obtained from *in vivo* MRI scanning were quantified at 2

different distances from Bregma, and showed low variability ($n = 4$ per experimental group). (B) EPM 1 week: prior to treatment at 7 days poststroke the 3 randomized stroke groups (PSD) compared with sham control showed anxiety phenotype with significantly reduced open-arm duration in EPM. (C) EPM 4 weeks: PSD reduced open-arm time compared with sham, indicative of an anxiety phenotype; this was reversed by chronic 3-week treatment with FLX (PSD/FLX) but not exercise (PSD/RW). As control for locomotion, total distance travelled did not differ between groups. (D) OF: PSD reduced large center duration and FLX or exercise reversed this anxiety phenotype, with no change in distance travelled. (E) NSF: PSD increased latency to feed in open field, and FLX but not exercise reversed this phenotype. As control for hunger, the latency to feed in home cage did not differ between groups. (F) FST: immobility time in PSD vs sham group was increased indicating behavioral despair, and this was reversed by FLX but not exercise. (G) TS: immobility increase in PSD was reversed by FLX but not exercise. Data represent mean \pm SEM, $n = 8$ per group, * $p < 0.05$, ** $p < 0.01$

chewed the food or after 10 min had expired for the trial, the mice were removed from the arena. The mice were placed in

their home cage and the latency to feed and amount of food consumed in 5 min was measured.

Morris Water Maze Test

A cued version of the MWM was used to evaluate spatial learning and memory in PSD and PSD treated mice [26]. The maze used was a circular pool (132 cm diameter) filled with nontoxic, white-colored water ($24 \pm 1^\circ\text{C}$). The platform diameter was 10 cm and was located 24 cm from the edge of the pool, hidden 1 cm beneath the surface of the water. Each 1-min trial was started by placing a randomly chosen mouse in 1 of 4 quadrant starting locations in the pool with its head outward. If the mouse found the platform within 60 s, it was left to stay on the platform for 5 s; if it did not find the platform, it was gently guided to the platform by the experimenter. Between the trials, all mice were placed back in their home cages while tucked in a towel in order to avoid direct contact with the experimenter. All trials were tracked using an overhead video camera and recorded automatically by an Ethovision digital tracking system (Noldus) to assess path line and latency to escape from the water. Four trials daily were conducted on each mouse with a 30-min intertrial interval. Trials ran for 10 days, at which time the sham control group consistently reached the platform. On the next day (probe day), the platform was removed and the amount of time the mouse spent in the quadrant where the platform used to be was measured.

Statistical Analyses

All analyses were done using SPSS (IBM, Armonk, NY, USA) and GraphPad Prism version 6.00 for Windows (GraphPad Software, La Jolla, CA, USA). Data are expressed as mean \pm SEM. Data comparing the sham *versus* stroke mice or vehicle *versus* single treatment on one outcome measure were analyzed using an unpaired *t* test. Data comparing the immunopositive cell counts within 1 area were also analyzed using an unpaired *t* test. Statistical analyses were performed using 1-way analysis of variance when comparing data across different conditions. Post-hoc comparisons were made with Tukey's multiple comparisons test.

Results

Chronic FLX Treatment, But Not Exercise, Restores Behavioral Phenotypes in PSD Mouse

As described previously, adult male C57BL6 mice received an ischemic lesion in the left mPFC to generate the PSD mouse model [19]. At 4 days poststroke, the lesion was verified in a subset of mice using MRI (Fig. 1, timeline). The MRI data showed consistent size and location of lesions (Fig. 1A), with average volume of $0.89 \pm 0.04 \text{ mm}^3$ and occupying $10.5 \pm 0.3\%/300 \mu\text{m}$ section, similar to that observed previously

[19]. The anxiety phenotype was verified at 1 week poststroke using the EPM assay. Compared with sham control, the randomly assigned stroke groups showed significant reduction in open arm duration (Fig. 1B). Then, treatment was begun: FLX was administered orally to obtain a clinically relevant concentration as described [25], and exercise was free RW with FW as control. After 3 weeks of treatment, the mice were tested in anxiety and depression tests over 2 weeks while maintaining treatment. Compared with sham, the stroke mice displayed significant anxiety (EPM, OF, and NSF tests; Fig. 1C–E) and depression-like (FST, TST; Fig. 1F, G) behavior, consistent with our previous results [19]. Chronic FLX reversed the anxiety phenotype to sham control levels in all tests: it increased open arm time in the EPM, time in center in the OF, and reduced latency to feed in the NSF test. However, exercise had no effect in the EPM or NSF tests but did reverse time in center to sham levels in the OF test (Fig. 1D). As controls for locomotor activity, no change was seen in the distance travelled in the EPM or OF tests (Fig. 1C, D), nor in the latency to feed or food consumed (not shown) in the home cage in the NSF test (Fig. 1E). Thus, chronic FLX alone completely reversed the poststroke anxiety phenotype, whereas exercise had little effect. Similarly, chronic SSRIs but not exercise reversed the depression-like behavior in the FST and TST, reducing the immobility duration to sham control levels (Fig. 1F, G).

Cognitive Impairment in PSD Mouse: Reversal by Chronic FLX Treatment

Cognitive impairment, including decline in learning and memory, is common in patients with PSD. Since the mPFC is implicated in cognitive function, we tested whether spatial learning and memory were impaired in the PSD *versus* sham control mice using a 10-day MWM test (Fig. 2, timeline). Compared with test day 1, the sham controls show progressive reduction in time to reach the platform from day 5 onwards, whereas the PSD mice displayed no consistent improvement, indicating a complete inability to learn the task (Fig. 2A). The FLX-treated PSD displayed rapid response in 1 day, with initial improvement greater than sham controls (days 2–4), indicating more rapid learning. Exercised PSD mice showed no improvement compared with PSD mice, and displayed significantly longer latency compared with sham mice from day 4 onwards. On day 11, in the probe test with the platform removed, the PSD and exercised PSD mice showed a reduced time in the target quadrant *versus* the sham and FLX-treated PSD mice, which spent the majority of time in the correct quadrant (Fig. 2B, C), indicating that the FLX-treated mice retained spatial memory. In 2 other cohorts ($n = 20$) without the fixed wheel, we observed a similar impairment in spatial learning with minimal improvement in the MWM over 10 days (data not shown). Thus, in addition to the behavioral

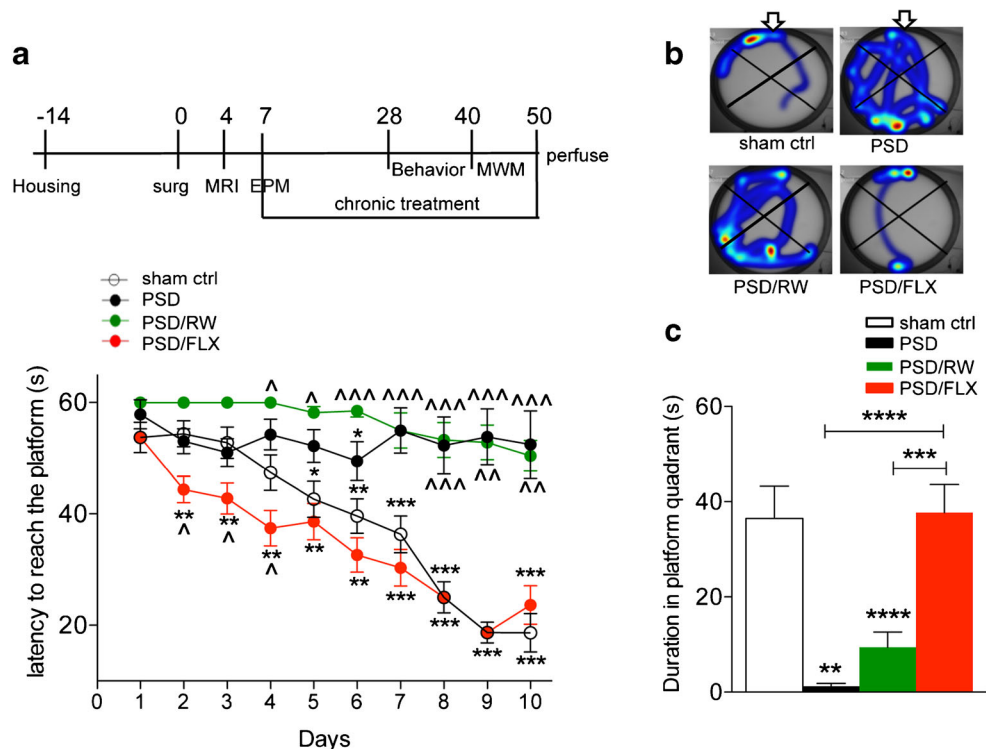


Fig. 2 Chronic fluoxetine (FLX), but not exercise, reverses spatial learning and memory in poststroke depression (PSD) mice. Spatial learning and memory were tested in the PSD mice treated with vehicle (PSD), FLX (PSD/FLX), or running wheel (RW) vs sham control (sham ctrl), with fixed wheel or vehicle as controls, using the Morris water maze (MWM; timeline, as in Fig. 1A). (A) Acquisition: the latency to reach the hidden platform was measured each test day. Compared with sham, the PSD and PSD/RW mice showed a nearly complete inability to locate the platform with the 60-s test, whereas the PSD/FLX mice showed a

significantly reduced latency to reach the platform from days 2 to 10, which was reduced compared with sham from days 2 to 4, suggesting enhanced spatial learning. (B) Probe test tracking: the search strategy taken by single mouse per experimental group in the probe test [arrow indicates the correct (upper) quadrant]. (C) Probe test. Compared with sham, PSD mice showed reduced duration in the target quadrant, and this was reversed in the PSD/FLX group but not in the PSD/RW mice. Data represent mean \pm SEM in $n = 8$ per group, * $p < 0.05$, ** $p < 0.01$, *** $p < 0.001$ vs. day 1, $\wedge p < 0.05$, $\wedge\wedge p < 0.01$, $\wedge\wedge\wedge p < 0.001$ vs sham ctrl

phenotype, ET-1-induced lesion in left mPFC is associated with cognitive impairment. Chronic FLX, but not exercise, reversed the poststroke impairment and enhanced spatial learning and memory capacity.

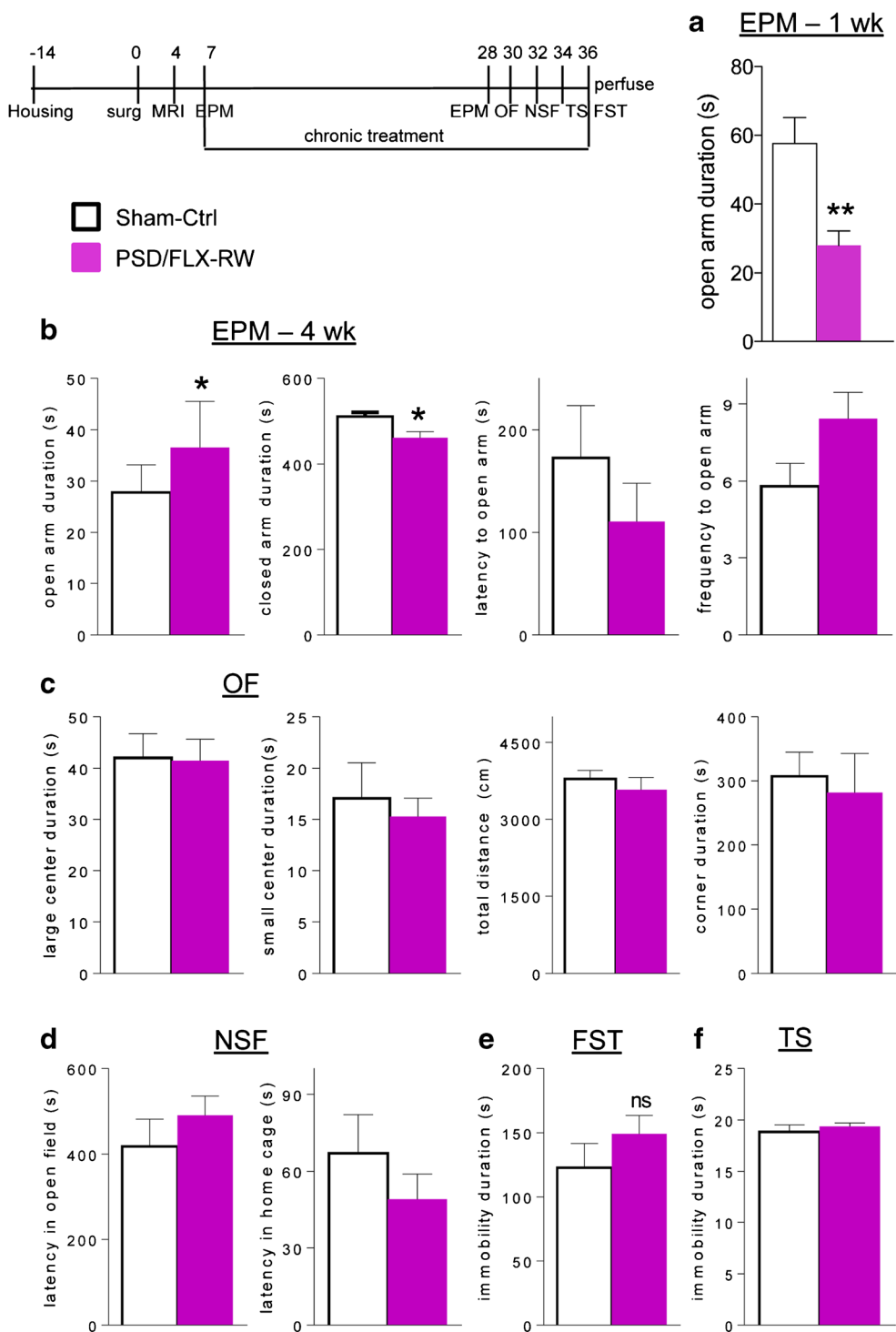
Combination FLX–Exercise Treatment Normalizes Behavior of PSD Mice

Stroke patients with PSD often receive physical rehabilitation and FLX as treatment. In the PSD mouse, we addressed whether there was any benefit to combining chronic FLX and exercise (Fig. 3). The strokes were verified by MRI with infarct volume of $0.97 \pm 0.08 \text{ mm}^3$ occupying $11.5 \pm 0.28\%$ of the 300- μm slice in MRI (mean \pm SE, $n = 4$). The anxiety phenotype of the stroke mice compared with sham control was verified before treatment at 1 week poststroke using the EPM assay (Fig. 3A). Interestingly, in the EPM test, at 4 weeks post-stroke combination treatment significantly increased open arm time and reduced corner time compared with sham control (Fig. 3B), suggesting an augmented antianxiety effect in this test compared with SSRI treatment alone. As observed

for chronic SSRI alone, combination treatment reversed the anxiety phenotype to sham control level in the OF and NSF tests (Fig. 3C, D) and also reversed depression-like behavior in the FST and TST to sham control levels (Fig. 3E, F). Thus, without or with exercise, chronic FLX treatment reversed the anxiety- and depression-like phenotypes in the PSD mouse.

Neuronal Activation in the mPFC–DR Circuitry Following PSD and Chronic Treatment

To address the effect of left mPFC stroke on brain activity, brain sections of corticolimbic areas (Fig. 4A; Table 2) were immunostained for FosB, a marker of chronic cellular activation [24, 27]. Using the cohort from our previous study (Fig. 4B) [19], the number of FosB-labeled cells was significantly increased in PSD compared with sham brains in several corticolimbic regions. These included the mPFC [cingulate gyrus (CG) and pre-/infralimbic (PI); Fig. 4B), nucleus accumbens (NAc), lateral septum (LSN) and lateral habenula (LHb), amygdala (Amy), ventral hippocampus (Hippo), dentate gyrus (DG), and the DR (Fig. 4C). In several of these



regions, this increase was significantly greater on the right compared with the left (ipsilesional) side, including the CG, PI, LSN, DG, and Amy (Fig. 4B, C). These results suggest that left mPFC ischemia chronically activates the mPFC and downstream limbic targets more on the right side.

The effect of chronic FLX *versus* exercise treatment on brain activity was evaluated using the first cohort of treated PSD mice (timeline, Fig. 1). To identify the cell types

activated, co-immunostaining for FosB with neuronal markers for 5-HT (TPH), glutamate (CAMKII α or VGluT), or γ -aminobutyric acid (GABA; GAD67) subtypes was quantified. In the DR, the number of FosB⁺ 5-HT, GABA, and glutamate cells increased from 4 days to 6 weeks poststroke (Fig. 5A, B). Notably, the total number of 5-HT cells, identified by TPH-positive staining, remained unchanged (Fig. 5C). Chronic FLX had little effect on the number of FosB/TPH⁺ cells but

Fig. 3 Combination fluoxetine (FLX)–exercise treatment normalizes behavior of poststroke depression (PSD) mice. Timeline: mice were individually housed (Housing) 14 days prior to surgery (surg), microinjected with vehicle (Sham-Ctrl) or endothelin 1 (ET-1; PSD) in the left medial prefrontal cortex (mPFC; surg, day 0); at 4 days poststroke, lesions were verified by magnetic resonance imaging (MRI), and at 7 days anxiety phenotype verified by elevated plus maze (EPM); from 7 days onwards PSD mice treated with the combination of FLX and running wheel (PSD/FLX-RW) were compared with sham-injected mice treated with vehicle and fixed wheel (Sham-Ctrl). (A) EPM 1 week: at 7 days poststroke, PSD mice had reduced open-arm time compared with sham, indicative of an anxiety phenotype. (B) EPM 4 weeks: after 3 weeks of combination treatment, the PSD/FLX-RW mice showed increased time spent in the open arms compared with sham, indicating reduced anxiety. There was no difference in latency or frequency to enter the open arm *vs* sham. (C) Open field (OF) test: PSD/FLX-RW mice showed similar times spent in both large and small center and in corner duration compared with sham, and the same total activity in open arena. (D) Novel suppressed feeding (NSF): no difference was seen in latency to approach food in new arena or to feed in home cage. (E) Forced swim test (FST): no difference in immobility time was seen between groups. (F) Tail suspension (TS) test: no difference in immobility time was seen between groups. Data represent mean \pm SEM; $n = 12$ per group, * $p < 0.05$; ** $p < 0.01$

induced FosB activity most prominently in TPH⁺ cells (Fig. 5A, yellow arrow). FLX significantly increased the number of FosB/GAD67⁺ cells in the DR (Fig. 5B, yellow arrow). In contrast, exercise greatly reduced FosB/GAD67⁺ cells, whereas the number of FosB/vGluT3⁺ cells remained high (Fig. 5D). Thus, chronic FLX recruited GABAergic raphe cells while maintaining the activation of 5-HT neurons.

To address whether brain activity changes seen poststroke were initiated early or late, we compared FosB-stained cells in brains from vehicle-treated PSD mice at 4 days or 6 weeks poststroke (Fig. 6 and Fig. S1, shown as a heat map in Fig. 7). At 4 days poststroke, the left mPFC shows no cells [19], and hence no FosB staining was observed in left CG/PI. At 6 weeks poststroke when the lesion is refilled with cells [19], FosB-stained cells were strongly increased. Compared with 4 days, in PSD mice at 6 weeks poststroke FosB-labeled cells were significantly induced in several brain regions (CG, PI, NAc; right CA2, CA3, and DG), but not in LHb, LSN, Amy, or in left CA2, CA3, or DG. The most prominent increases were in FosB/CAMKII-labeled cells, in the mPFC (CG and PI), NAc, LSN, and right CA2, CA3, and DG, suggesting a hyperactivation of pyramidal neurons in the corticolimbic circuitry. By contrast, in the LHb mainly GABAergic cells were activated, consistent with their inverse activity in depression phenotypes [28].

Chronic FLX treatment induced distinct changes in FosB-stained cells compared with vehicle- or exercise-treated PSD groups (Figs 6 and 7, Fig. S1). In regions where PSD (6 weeks) increased FosB-stained cells (CG, NAc), FLX, and combination treatment but not exercise strongly reduced FosB, especially on the right side to balance left–right activity (Fig. 7, Fig. S1). In these areas, PSD increased

FosB/CAMKII⁺ neurons at 6 weeks *versus* 4 d (CG, PI, NAc, CA3, DG) and chronic FLX and exercise strongly reduced these changes (Fig. 6). In regions where PSD did not strongly induce FosB, FLX and combination treatments but not exercise bilaterally induced FosB-stained (LSN, Amy) and FosB/GAD67-stained cells (LSN) (Figs 6 and 7, Fig. S1). Chronic FLX but not exercise also increased FosB/GAD67⁺ cells on the left side in PI, NAc, and Amy, as well as in the right hippocampal CA2 and CA3 regions. In these regions, exercise alone often had opposite effects to reduce ipsilateral GABAergic or increase contralateral glutamatergic activation, reversing the left–right balance. Thus, in key areas implicated in anxiety (LSN/Amy) and depression (mPFC, NAc), chronic FLX enhanced the activity of GABAergic inhibitory neurons or reduced the activity pyramidal neurons, respectively, to balance left–right activity ratio.

The combination of chronic FLX/exercise (separate cohort, Fig. 3) uniquely and strongly induced FosB⁺ and FosB/GAD67⁺ in the hippocampal DG (bilateral) and increased left DG FosB/CAMKII-labeled cells (Fig. 7, S1). Thus, compared with FLX alone, the combination appears to preferentially target the DG, which is implicated in anxiety and depression, spatial memory, and adult neurogenesis, to produce behavior improvements.

Discussion

Chronic FLX Promotes Recovery From PSD Phenotypes

Current treatments for PSD, including chronic antidepressant treatment, are not effective in many patients. In order to provide insight into effective treatments for PSD and associated anxiety and cognitive impairments, we have taken advantage of our PSD mouse model. Evidence from human imaging studies suggests that alterations in the activity of the mPFC–DR limbic circuitry are associated with anxiety disorders and major depression [22, 29, 30]. Therefore, we targeted mPFC as a central node of the mPFC–subcortical limbic circuitry [31] to model PSD phenotypes [32, 33]. While lesion of the mPFC from anterior cerebral artery stroke is rare, much more common large ischemic or white-matter strokes appear to disrupt multiple nodes and connections within the anxiety–depression circuitry, resulting in PSD [34, 35]. Previous rodent models of PSD have used large MCAO strokes, but required combination with chronic mild stress to elicit depression and cognitive phenotypes [36]. Hence, these provide mixed models of stress- and ischemia-induced phenotypes, whereas our mPFC lesion selectively models ischemia-induced behavioral and cognitive outcomes. Thus, it remains unclear whether SSRI treatment in these mixed models ameliorates poststroke or stress-induced depression [37] or affects anxiety

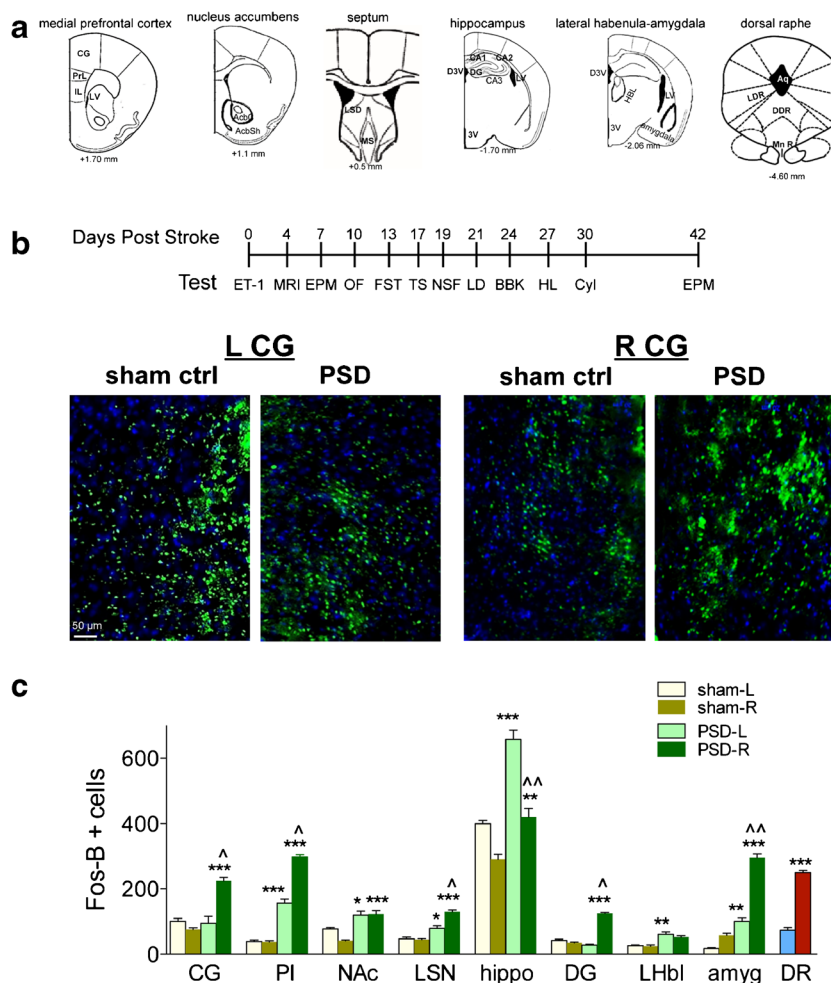


Fig. 4 Effect of stroke on FosB⁺ cells in corticolimbic brain areas. Following behavioral assays at 6 weeks poststroke and 1 day following the last assay mice were perfused, brains sections and immunostained for FosB, and the number of FosB⁺ cells quantified in regions where activation was seen. (A) Schematic representation of the brain sections in which FosB activity was observed. (B) Above: timeline for the sham vs poststroke depression (PSD) cohort of mice [19]. Below: representative photomicrographs of FosB immunofluorescence (green) and 4',6-diamidino-2-phenylindole (blue) in cingulate gyrus (CG), left (L) vs right (R) in sham ctrl and PSD. Images were taken under 20 \times magnification,

scale bar = 20 μ m. (C) Quantification of FosB⁺ cells. FosB⁺ cells were quantified in the left (L) and right (R) sides, and were increased in PSD vs sham control in right CG and pre-/infralimbic areas (PI) of medial prefrontal cortex, hippocampus (hippo), nucleus accumbens (NAc), lateral septum (LSN), amygdala (amyg), lateral habenula (LHbl), and dorsal raphe (DR) compared with sham control. In several areas, FosB⁺ cells were significantly more increased in right vs left side in the PSD group. Data represent mean \pm SEM in $n = 4$ per group, * $p < 0.05$, ** $p < 0.01$, *** $p < 0.001$ vs sham ctrl, $\wedge p < 0.05$, $\wedge\wedge p < 0.01$ vs contralateral side

or cognitive function. Furthermore, while SSRIs are partly effective to treat of major depression and PSD in the clinic [11, 38], it remains unclear whether anxiety, depression, and cognitive function are improved, and why some patients fail to respond. Since the anxiety and depression phenotype of our PSD mouse model persists for at least 6 weeks [19], we addressed the effect of chronic treatments. We found that, in the PSD mouse, chronic FLX alone fully reversed both anxiety and depression phenotypes, as well as cognitive function, suggesting that this treatment can reverse ischemia-induced behavioral and cognitive deficits in patients.

In the PSD mouse, we find severe deficits in spatial learning and memory in the MWM assay. In contrast to unilateral ischemia, others have shown that bilateral ET-1-induced

stroke in rodent mPFC induces impairments in spatial learning but with a subtle effect on anxiety behavior [39–41]. Compared with bilateral strokes, unilateral mPFC lesion may disinhibit the contralateral mPFC to drive the behavioral phenotype, as suggested by our FosB activation data. Consistent with this, some evidence suggests that left but not right MCAO in rats induced depression and anxiety-like behavior [37]. Clinical studies suggest that unilateral ischemia affecting the left mPFC is preferentially associated with PSD [11, 42, 43], although the opposite has also been seen [44]. Ischemia of the left PFC is also associated with cognitive impairment [45, 46], indicating the usefulness of unilateral lesions in mouse mPFC to model poststroke cognitive impairment. In addition to behavioral improvement, we demonstrate

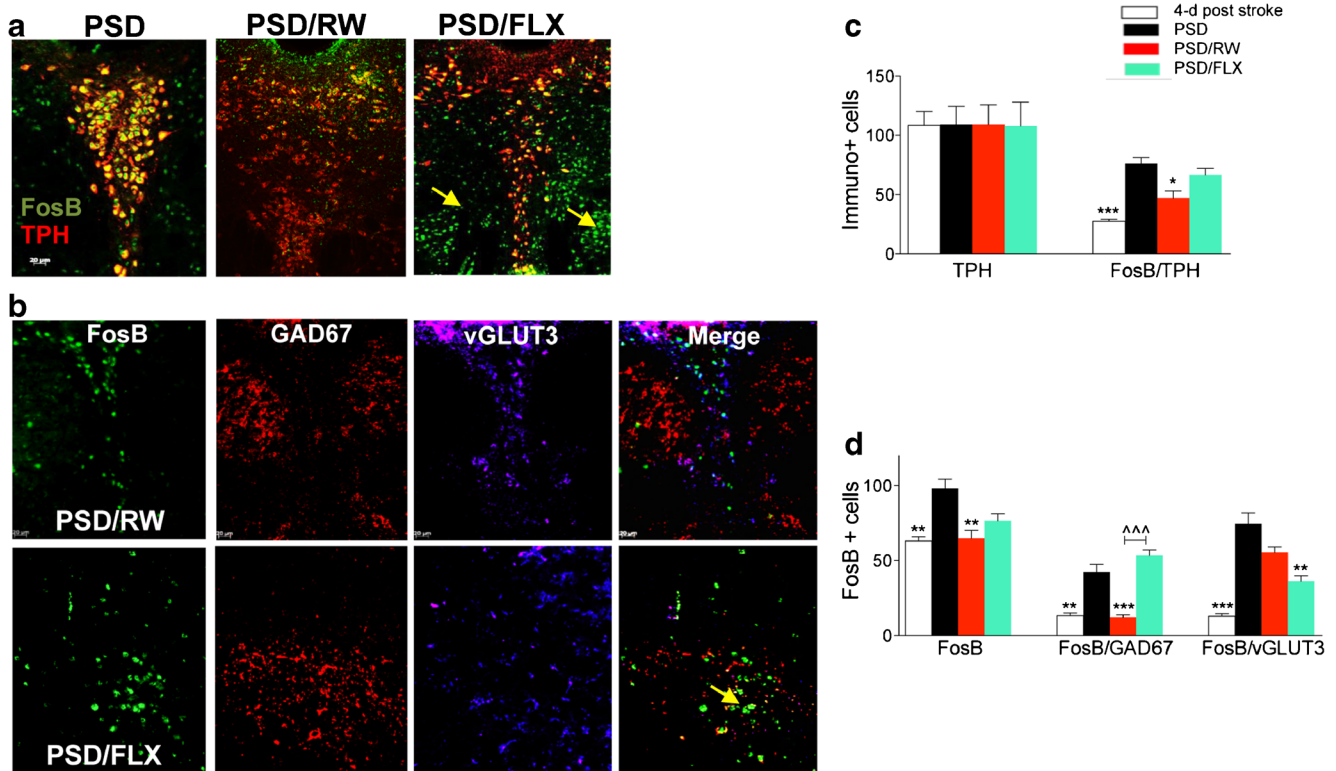


Fig. 5 Chronic treatment-induced changes in FosB⁺ dorsal raphe cells. Sections of dorsal raphe (DR) were prepared from control poststroke depression (PSD) mice at 4 days poststroke or 6 weeks poststroke or from PSD mice (6 weeks poststroke) treated with running wheel (PSD/RW) or fluoxetine (PSD/FLX). The sections were stained for FosB, tryptophan hydroxylase (TPH), GAD67, and VGLUT3 to identify FosB-positive serotonin (5-HT), γ -aminobutyric acidergic, and glutamatergic neurons. (A) FosB/TPH co-staining. Merged images show FosB (green), TPH (red), and co-stained (yellow) cells in dorsal raphe. Arrows show TPH⁺FosB⁺ cells [possibly GABAergic, see (B) in ventrolateral DR]. Images were taken under 40 \times magnification. Scale bar = 50 μ m. (B) FosB–GAD67–VGLUT3 co-staining in PSD/RW vs PSD/FLX DR. Images of FosB (green), GAD67 (red), VGLUT3 (magenta), and merged

images, 20 \times magnification, scale bar = 20 μ m. Arrow shows FosB⁺ only cells in PSD/FLX-treated samples. PSD/FLX induced higher activation of GAD67⁺ cells in DR (FosB/GAD67) compared to VGLUT3 positive cells in DR, while PSD/RW induced higher activation of VGLUT3 positive cells in DR. (C) Quantification of total TPH⁺ and FosB/TPH immune-positive (Immu⁺) cells in DR. Exercise reduced the number of FosB/TPH⁺ cells (PSD/RW vs PSD), whereas PSD/FLX showed no change. (D) Quantification of FosB⁺, FosB/GAD67⁺, and FosB/VGLUT3⁺ cells in dorsal raphe. Compared with control (PSD/FW), in PSD/RW mice but not PSD/FLX mice, a reduction in FosB/GAD67⁺ cells was seen. Data represent mean \pm SEM in $n = 4$ per group, * $p < 0.05$, ** $p < 0.01$, *** $p < 0.001$ vs PSD/FW. ^^ $p < 0.001$ vs other groups as indicated by bars; 2-way analysis of variance (Tukey's post-hoc)

that chronic FLX, but not exercise, strongly reverses the poststroke cognitive impairment in these mice. This finding suggests that chronic SSRI treatment of patients with PSD may enhance cognitive recovery, in agreement with clinical studies [11, 38], particularly in patients with strokes that affect PFC function [9]. In summary, these findings highlight the potential benefits of chronic FLX poststroke, not only to treat anxiety and depression, but also to improve cognitive recovery.

Unexpectedly, we found that while chronic FLX treatment reversed poststroke anxiety, depression, and cognitive phenotypes in the PSD mouse, exercise had minimal benefit on its own. However, the combination of SSRI and exercise was effective, and even reduced anxiety to below sham control levels in the OF test. Like chronic FLX, free-running wheel exercise may have beneficial effects in ischemic animals, such as enhancing brain growth factors, hippocampal neurogenesis and angiogenesis [47–49]. In mice, running mediates the

neurogenic and neurotrophic effects of enriched environment [50]. Both chronic SSRI and exercise increase hippocampal neurogenesis in mice post-MCAO associated with improvement in the MWM test [15, 51]. Targeted exercise can also enhance poststroke cortical plasticity and sensorimotor recovery [52], and intense exercise may have a mildly beneficial effect in PSD recovery in stroke patients [53]. However, early (within a week poststroke) rehabilitation can actually be detrimental to functional recovery [54]. The use of exercise combined with SSRI for PSD has been suggested in humans [53], but the combination of FLX and exercise had little added benefit compared to FLX alone in our PSD mouse model.

Chronic FLX Reverses Stroke-Induced Imbalance in Neuronal Activation

To provide insight into the chronic changes in brain activity following unilateral ischemic lesion and treatment, we

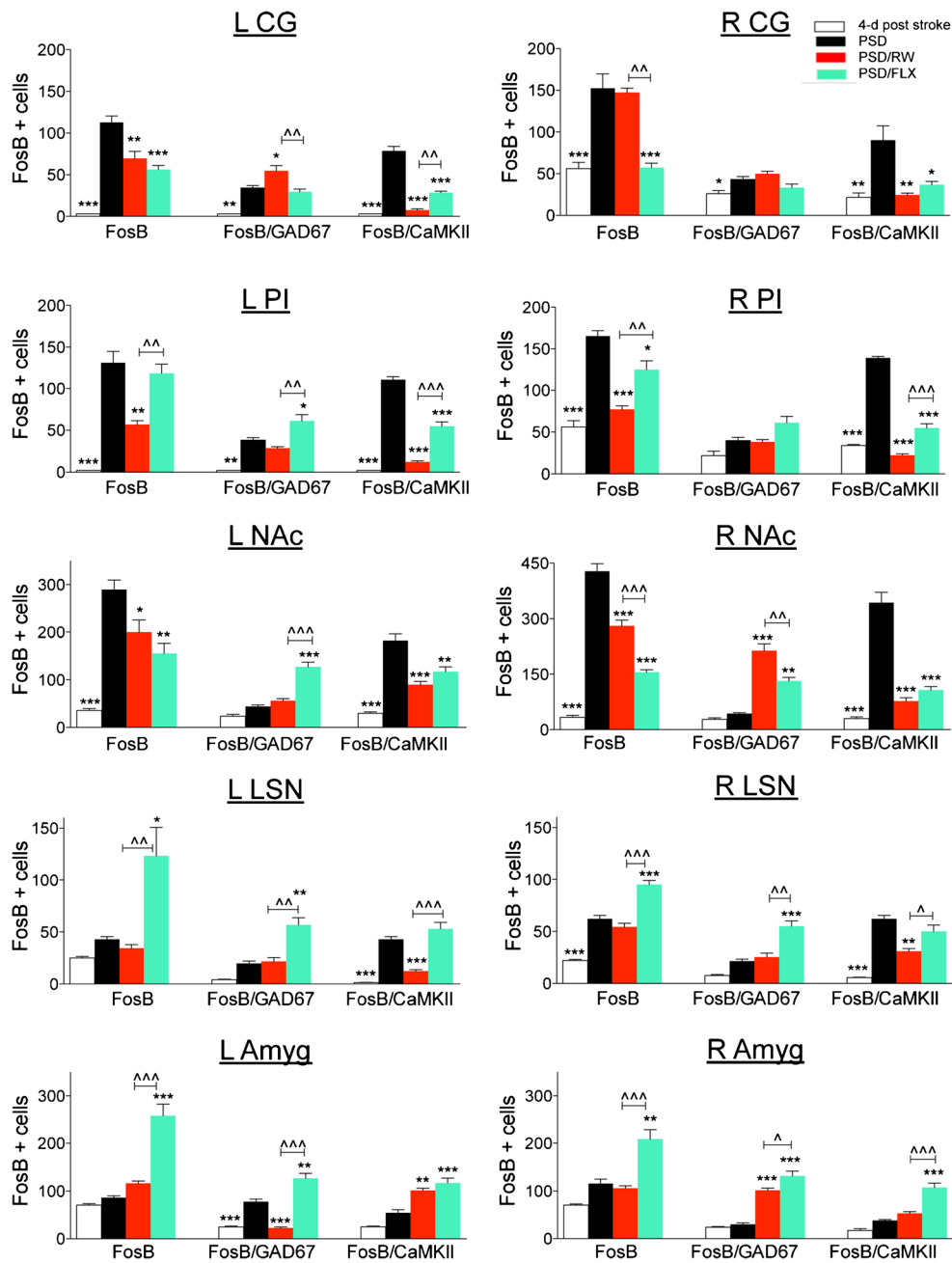


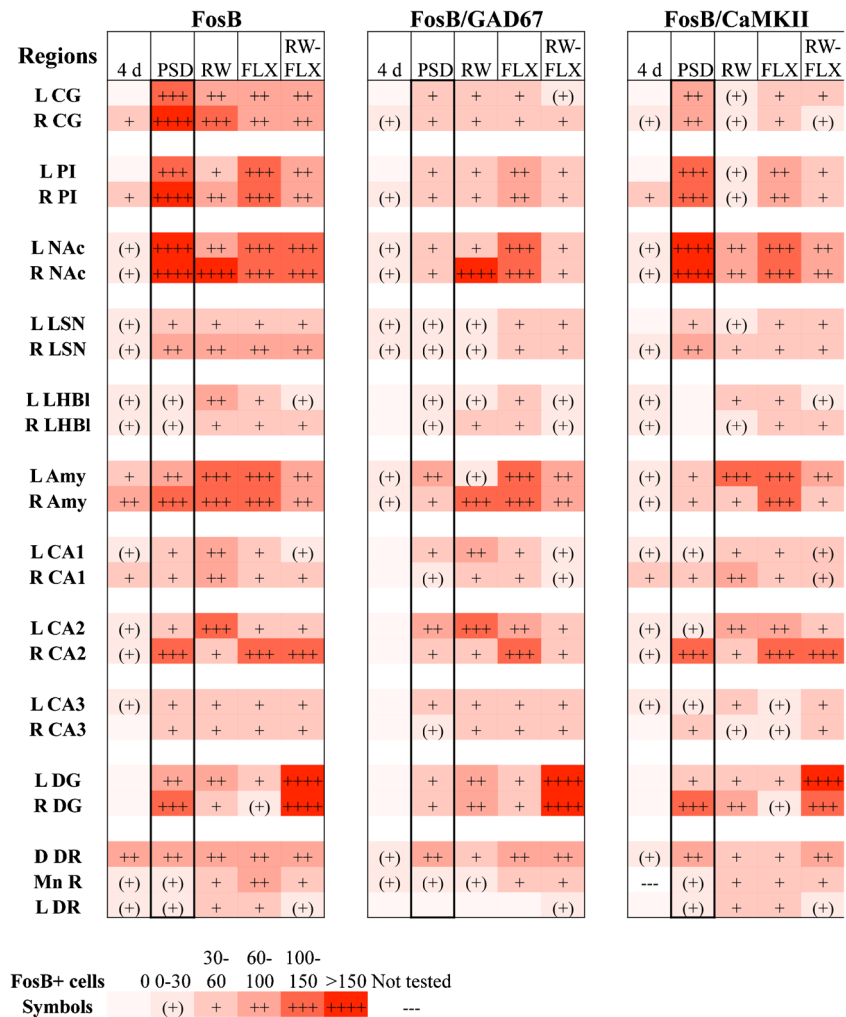
Fig. 6 Chronic treatment-induced changes in FosB⁺ cells and cell types in poststroke depression (PSD) mice. Sections were prepared from PSD mice at 4 days poststroke (4 d) or at 6 weeks poststroke after control (vehicle/ fixed wheel, PSD), fluoxetine/ fixed wheel (PSD/FLX), or running wheel (PSD/RW) chronic treatments (see timeline in Fig. 1). Sections were co-stained for FosB, GAD67, and CaMKII and total FosB₊ (FosB), FosB⁺ γ -aminobutyric acidergic (FosB/GAD67), or pyramidal (FosB/CaMKII) neurons were quantified on ipsilateral left (L) and contralateral right (R) side. Shown is data from medial prefrontal cortex (CG = cingulate gyrus; PI = pre-/infralimbic cortex; nucleus accumbens = NAc; lateral septum = LSN; Amyg = amygdala = Amyg). Compared with

PSD/FW (at 6 weeks), at 4 days poststroke, no FosB was detected in left CG-PI, consistent with absence of cells acutely following the lesion, whereas FosB was very low in right CG-PI and in NAc. Comparing treated with vehicle-treated PSD mice, CG-PI-NAc showed similar patterns of reductions in FosB⁺ and FosB/CaMKII⁺ cells, whereas LSN-Amyg showed increases in FosB⁺ and FosB/GAD67⁺ cells, especially for effective treatment (FLX). Data represent mean \pm SEM in $n = 4$ per group, * $p < 0.05$, ** $p < 0.01$, *** $p < 0.001$ vs PSD/FW. $\wedge p < 0.05$, $\wedge\wedge p < 0.01$, $\wedge\wedge\wedge p < 0.001$ vs other group as indicated by bars; 2-way analysis of variance (Tukey's post-hoc)

mapped FosB⁺ cells. Compared with other methods, such as calcium imaging or electrophysiology that provide a snapshot of activity at a given time, FosB staining integrates activity

over a chronic period of time, providing an average overall activity readout [24]. However, we cannot rule out activation of other regions that do not express FosB, and thus we could

Fig. 7 Heat map of chronic treatment-induced changes in FosB⁺ cells and cell types in poststroke depression (PSD) mice. Data on the number of FosB⁺ cells from Fig. S1 were plotted as a heat map with cell count ranges shown in the legend below. The cell counts are based on the number of total FosB, FosB/GAD67, or FosB/CAMKII (VGluT3 for raphe) stained cells from PSD mice at 4 days poststroke (4 d) or at 6 weeks poststroke after treatments: control (vehicle/fixated wheel, PSD) fluoxetine/fixated wheel (FLX), running wheel (RW), or combination FLX and RW (FLX-RW). Shown are left (L) and right (R): CG = cingulate gyrus; PI = pre-/infralimbic cortex; NAc = nucleus accumbens; LSN = lateral septum; LHBI = lateral habenula; Amy = amygdala; hippocampal CA1, CA2, CA3; DG = dentate gyrus; D DR = dorsal raphe, dorsal; L DR = lateral wings; Mn R = median raphe



not detect changes in activity in these regions. Furthermore, the observed changes in FosB could be due, in part, to secondary changes in activity associated with behavioral or cognitive alterations.

We found that brain-wide FosB activity was relatively low at 4 days poststroke. At 6 weeks poststroke there was a parallel increase in the activity of the mPFC and several of its limbic and raphe targets compared with 4 days poststroke and to sham control, consistent with the emergence of the behavioral phenotype. Similarly, following ET-1-induced ischemia in rat sensorimotor cortex, FosB-labeled cells increased between 9 and 17 days postischemia in contralesional cortex and perilesional striatal regions [55]. Thus, the acute silencing of FosB activity at 4 days poststroke appears to transition to a hyperactivated state that may drive the behavioral phenotype. In agreement, the PSD mice displayed a greater number of FosB/CaMKII⁺ pyramidal cells at 6 weeks *versus* 4 d in the mPFC, NAc, LSN, and hippocampal regions (CA3, DG) (Figs 6 and 7). Importantly, ischemia of the left mPFC resulted in a preferential activation of the contralateral right brain, including the right mPFC, NAc, amygdala, and LSN (Fig. 4C). This

suggests a contralateral inhibition model similar to that proposed for left motor cortex lesions [56, 57]. In the left motor cortex lesion, the loss of projections from the left side disinhibits the right side, which is propagated to its targets.

Chronic FLX treatment reduced total FosB⁺ cells and FosB in pyramidal cells in the mPFC and NAc, reversing the effect of PSD. An analogous effect of FLX to reduce PFC activity is observed in human depression [58]. In the NAc, chronic antidepressant treatment increases FosB levels in stressed mice; however, the induced FosB is rendered inactive [27, 59]. This is consistent with an antidepressant effect of reduced NAc FosB activity that we observed in the recovered PSD mice. Conversely, in regions implicated in anxiety (LSN/Amy), effective treatments increased FosB⁺ cells, whereas exercise did not (Fig. 7, Fig. S1). This suggests that these regions were recruited by FLX treatment to restore the PSD behavioral phenotype. The lateral septum receives dense 5-HT innervation and is particularly sensitive to SSRIs [60, 61]. In PSD mice, chronic FLX and combination treatments but not exercise alone induced GABAergic FosB⁺ cells, consistent with a chronic anxiolytic role for septal interneurons [62–64]. A

similar response to FLX was seen in the Amy, driven in part by increased GABAergic activation, which may also mediate an antianxiety effect [65, 66].

In the DR, we found that chronic FLX and combination treatment increased raphe GABAergic activation compared with exercise. In fact, raphe GABAergic interneurons respond to aversive stimuli and act locally to inhibit 5-HT neurons [67]. In addition, some raphe GABAergic neurons project to the mPFC and NAc and may reduce forebrain activation [68]. In the raphe, chronic FLX failed to increase FosB/TPH⁺ neurons, which may reflect compensatory autoinhibition by 5-HT_{1A} receptors in the presence of SSRI treatment. However, chronic FLX treatment reduced FosB/VGluT3⁺ neurons. This may represent deactivation of raphe 5-HT/glutamate neurons, which have been shown to activate hippocampal interneurons [69] and could contribute to the behavioral effect of chronic FLX treatment.

In summary, while PSD leads to a lateralized activation pyramidal cells of the right mPFC and several limbic targets, effective treatments selectively reversed these changes to balance left *versus* right side activation, partially reducing pyramidal cell activation in the mPFC and NAc. Furthermore, effective treatments but not exercise targeted GABAergic cells within the lateral septum, amygdala and raphe to reduce pyramidal neuron activation and normalize behavior. Future optogenetic studies to directly target these neuronal populations could address their role in poststroke behavioral recovery.

Conclusion

Several important findings arise from our studies of the PSD mouse model: first, chronic FLX but not exercise alone reversed both anxiety and depression phenotypes; second, the PSD mice showed a pronounced cognitive impairment that was reversed by FLX but not exercise; and third that combination of FLX and exercise was effective for behavioral recovery but not more effective than FLX alone. Chronic FLX treatment preferentially activated GABAergic neurons in the LSN and Amy, and partially inhibited cortical and accumbens neurons activated following the stroke. The neuromodulatory effects of chronic SSRI treatment may underlie a broad benefit in enhancing stroke recovery observed in stroke patients [10, 70].

Acknowledgements We thank Dr. Ania Serefko, Danika Cziranka-Crooks, Rosalie Gauthier, and Mirela Barclay for technical assistance with parts of the research. We thank Drs. Dale Corbett and Baptiste Lacoste, University of Ottawa, for helpful comments on the manuscript. This research was supported by grants to P.R.A. from the Canadian Partnership for Stroke Recovery (CPSR) and the Canadian Institutes of Health Research. F.V.A. was supported by a CPSR studentship award.

References

1. Paolucci S, Gandolfo C, Provinciali L, Torta R, Toso V. The Italian multicenter observational study on post-stroke depression (DESTRO). *J Neurol* 2006;253:556-562.
2. Ayerbe L, Ayis S, Crichton S, Wolfe CD, Rudd AG. The natural history of depression up to 15 years after stroke: the South London Stroke Register. *Stroke* 2013;44:1105-1110.
3. Wolfe CD, Crichton SL, Heuschmann PU, et al. Estimates of outcomes up to ten years after stroke: analysis from the prospective South London Stroke Register. *PLOS Med* 2011;8:e1001033.
4. Galligan NG, Hevey D, Coen RF, Harbison JA. Clarifying the associations between anxiety, depression and fatigue following stroke. *J Health Psychol* 2016;21:2863-2871.
5. Ayerbe L, Ayis S, Crichton SL, Rudd AG, Wolfe CD. Explanatory factors for the increased mortality of stroke patients with depression. *Neurology* 2014;83:2007-2012.
6. Pompili M, Venturini P, Lamis DA, et al. Suicide in stroke survivors: epidemiology and prevention. *Drugs Aging* 2015;32:21-29.
7. Mead GE, Hsieh CF, Lee R, et al. Selective serotonin reuptake inhibitors (SSRIs) for stroke recovery. *Cochrane Database Syst Rev* 2012;11:CD009286.
8. Jorge RE, Acion L, Moser D, Adams HP, Jr., Robinson RG. Escitalopram and enhancement of cognitive recovery following stroke. *Arch Gen Psychiatry* 2010;67:187-196.
9. Flaster M, Sharma A, Rao M. Poststroke depression: a review emphasizing the role of prophylactic treatment and synergy with treatment for motor recovery. *Top Stroke Rehabil* 2013;20:139-150.
10. Chollet F, Tardy J, Albucher JF, et al. Fluoxetine for motor recovery after acute ischaemic stroke (FLAME): a randomised placebo-controlled trial. *Lancet Neurol* 2011;10:123-130.
11. Robinson RG, Jorge RE. Post-stroke depression: a review. *Am J Psychiatry* 2016;173:221-231.
12. Mortensen JK, Larsson H, Johnsen SP, Andersen G. Impact of prestroke selective serotonin reuptake inhibitor treatment on stroke severity and mortality. *Stroke* 2014;45:2121-2123.
13. Rimer J, Dwan K, Lawlor DA, et al. Exercise for depression. *Cochrane Database Syst Rev* 2012;7:CD004366.
14. Duman CH, Schlesinger L, Russell DS, Duman RS. Voluntary exercise produces antidepressant and anxiolytic behavioral effects in mice. *Brain Res* 2008;1199:148-158.
15. Luo CX, Jiang J, Zhou QG, et al. Voluntary exercise-induced neurogenesis in the posts ischemic dentate gyrus is associated with spatial memory recovery from stroke. *J Neurosci Res* 2007;85:1637-1646.
16. Greenwood BN, Foley TE, Day HE, et al. Freewheel running prevents learned helplessness/behavioral depression: role of dorsal raphe serotonergic neurons. *J Neurosci* 2003;23:2889-2898.
17. Castren E, Hen R. Neuronal plasticity and antidepressant actions. *Trends Neurosci* 2013;36:259-267.
18. Ayerbe L, Ayis SA, Crichton S, Rudd AG, Wolfe CD. Explanatory factors for the association between depression and long-term physical disability after stroke. *Age Ageing* 2015;44:1054-1058.
19. Vahid-Ansari F, Lagace DC, Albert PR. Persistent post-stroke depression in mice following unilateral medial prefrontal cortical stroke. *Transl Psychiatry* 2016;6:e863.
20. Kronenberg G, Gertz K, Heinz A, Endres M. Of mice and men: modelling post-stroke depression experimentally. *Br J Pharmacol* 2014;171:4673-4689.
21. Albert PR, Vahid-Ansari F, Luckhart C. Serotonin-prefrontal cortical circuitry in anxiety and depression phenotypes: pivotal role of pre- and post-synaptic 5-HT_{1A} receptor expression. *Front Behav Neurosci* 2014;8:199.

22. Ressler KJ, Mayberg HS. Targeting abnormal neural circuits in mood and anxiety disorders: from the laboratory to the clinic. *Nat Neurosci* 2007;10:1116-1124.
23. Calhoun GG, Tye KM. Resolving the neural circuits of anxiety. *Nat Neurosci* 2015;18:1394-1404.
24. Nestler EJ. FosB: a transcriptional regulator of stress and antidepressant responses. *Eur J Pharmacol* 2015;753:66-72.
25. Dulawa SC, Holick KA, Gundersen B, Hen R. Effects of chronic fluoxetine in animal models of anxiety and depression. *Neuropsychopharmacology* 2004;29:1321-1330.
26. Vorhees CV, Williams MT. Morris water maze: procedures for assessing spatial and related forms of learning and memory. *Nat Protoc* 2006;1:848-858.
27. Vialou V, Thibault M, Kaska S, et al. Differential induction of FosB isoforms throughout the brain by fluoxetine and chronic stress. *Neuropharmacology* 2015;99:28-37.
28. Warden MR, Selimbeyoglu A, Mirzabekov JJ, et al. A prefrontal cortex-brainstem neuronal projection that controls response to behavioural challenge. *Nature* 2012;492:428-432.
29. Krishnan V, Nestler EJ. The molecular neurobiology of depression. *Nature* 2008;455:894-902.
30. Northoff G, Wiebking C, Feinberg T, Panksepp J. The 'resting-state hypothesis' of major depressive disorder—a translational subcortical-cortical framework for a system disorder. *Neurosci Biobehav Rev* 2011;35:1929-1945.
31. Riga D, Matos MR, Glas A, Smit AB, Spijker S, Van den Oever MC. Optogenetic dissection of medial prefrontal cortex circuitry. *Front Syst Neurosci* 2014;8:230.
32. Singh A, Black SE, Herrmann N, et al. Functional and neuroanatomic correlations in poststroke depression: the Sunnybrook Stroke Study. *Stroke* 2000;31:637-644.
33. Yang S, Hua P, Shang X, et al. A significant risk factor for poststroke depression: the depression-related subnetwork. *J Psychiatry Neurosci* 2015;40:259-268.
34. Lassalle-Lagadec S, Sibon I, Dilharreguy B, Renou P, Fleury O, Allard M. Subacute default mode network dysfunction in the prediction of post-stroke depression severity. *Radiology* 2012;264:218-224.
35. Liao Y, Huang X, Wu Q, et al. Is depression a disconnection syndrome? Meta-analysis of diffusion tensor imaging studies in patients with MDD. *J Psychiatry Neurosci* 2013;38:49-56.
36. Kim YR, Kim HN, Pak ME, et al. Studies on the animal model of post-stroke depression and application of antipsychotic aripiprazole. *Behav Brain Res* 2015;287:294-303.
37. Kronenberg G, Balkaya M, Prinz V, et al. Exofocal dopaminergic degeneration as antidepressant target in mouse model of poststroke depression. *Biol Psychiatry* 2012;72:273-281.
38. Zhang LS, Hu XY, Yao LY, et al. Prophylactic effects of duloxetine on post-stroke depression symptoms: an open single-blind trial. *Eur Neurol* 2013;69:336-343.
39. Deziel RA, Ryan CL, Tasker RA. Ischemic lesions localized to the medial prefrontal cortex produce selective deficits in measures of executive function in rats. *Behav Brain Res* 2015;293:54-61.
40. Livingston-Thomas JM, Jeffers MS, Nguemeni C, Shoichet MS, Morshead CM, Corbett D. Assessing cognitive function following medial prefrontal stroke in the rat. *Behav Brain Res* 2015;294:102-110.
41. Zhou LY, Wright TE, Clarkson AN. Prefrontal cortex stroke induces delayed impairment in spatial memory. *Behav Brain Res* 2016;296:373-378.
42. Murakami T, Hama S, Yamashita H, et al. Neuroanatomic pathways associated with poststroke affective and apathetic depression. *Am J Geriatr Psychiatry* 2013;21:840-847.
43. Terroni L, Amaro E, Iosifescu DV, et al. Stroke lesion in cortical neural circuits and post-stroke incidence of major depressive episode: a 4-month prospective study. *World J Biol Psychiatry* 2011;12:539-548.
44. Wei N, Yong W, Li X, et al. Post-stroke depression and lesion location: a systematic review. *J Neurol* 2015;262:81-90.
45. Potter GG, Blackwell AD, McQuoid DR, et al. Prefrontal white matter lesions and prefrontal task impersistence in depressed and nondepressed elders. *Neuropsychopharmacology* 2007;32:2135-2142.
46. Bolla-Wilson K, Robinson RG, Starkstein SE, Boston J, Price TR. Lateralization of dementia of depression in stroke patients. *Am J Psychiatry* 1989;146:627-634.
47. Will B, Galani R, Kelche C, Rosenzweig MR. Recovery from brain injury in animals: relative efficacy of environmental enrichment, physical exercise or formal training (1990–2002). *Prog Neurobiol* 2004;72:167-182.
48. Swain RA, Harris AB, Wiener EC, et al. Prolonged exercise induces angiogenesis and increases cerebral blood volume in primary motor cortex of the rat. *Neuroscience* 2003;117:1037-1046.
49. Kleim JA, Cooper NR, VandenBerg PM. Exercise induces angiogenesis but does not alter movement representations within rat motor cortex. *Brain Res* 2002;934:1-6.
50. Kobil T, Liu QR, Gandhi K, Mughal M, Shaham Y, van Praag H. Running is the neurogenic and neurotrophic stimulus in environmental enrichment. *Learn Mem* 2011;18:605-609.
51. Li WL, Cai HH, Wang B, et al. Chronic fluoxetine treatment improves ischemia-induced spatial cognitive deficits through increasing hippocampal neurogenesis after stroke. *J Neurosci Res* 2009;87:112-122.
52. Overman JJ, Carmichael ST. Plasticity in the injured brain: more than molecules matter. *Neuroscientist* 2014;20:15-28.
53. Eng JJ, Reime B. Exercise for depressive symptoms in stroke patients: a systematic review and meta-analysis. *Clin Rehabil* 2014;28:731-739.
54. Bernhardt J, Langhorne P, Lindley RI, et al. Efficacy and safety of very early mobilisation within 24 h of stroke onset (AVERT): a randomised controlled trial. *Lancet* 2015;386:46-55.
55. Clarke J, Langdon KD, Corbett D. Early poststroke experience differentially alters periinfarct layer II and III cortex. *J Cereb Blood Flow Metab* 2014;34:630-637.
56. Dijkhuizen RM, Singhal AB, Mandeville JB, et al. Correlation between brain reorganization, ischemic damage, and neurologic status after transient focal cerebral ischemia in rats: a functional magnetic resonance imaging study. *J Neurosci* 2003;23:510-517.
57. Silasi G, Murphy TH. Stroke and the connectome: how connectivity guides therapeutic intervention. *Neuron* 2014;83:1354-1368.
58. Komlosi G, Molnar G, Rozsa M, Olah S, Barzo P, Tamas G. Fluoxetine (prozac) and serotonin act on excitatory synaptic transmission to suppress single layer 2/3 pyramidal neuron-triggered cell assemblies in the human prefrontal cortex. *J Neurosci* 2012;32:16369-16378.
59. Robison AJ, Vialou V, Sun HS, et al. Fluoxetine epigenetically alters the CaMKIIalpha promoter in nucleus accumbens to regulate DeltaFosB binding and antidepressant effects. *Neuropsychopharmacology* 2014;39:1178-1186.
60. Hai A, Cai LX, Lee T, Lelyveld VS, Jasanoff A. Molecular fMRI of serotonin transport. *Neuron* 2016;92:754-765.
61. Sheehan TP, Chambers RA, Russell DS. Regulation of affect by the lateral septum: implications for neuropsychiatry. *Brain Res Brain Res Rev* 2004;46:71-117.
62. Parfitt GM, Nguyen R, Bang JY, et al. Bidirectional control of anxiety-related behaviors in mice: role of inputs arising from the ventral hippocampus to the lateral septum and medial prefrontal cortex. *Neuropsychopharmacology* 2017;42:1715-1728.
63. Trent NL, Menard JL. The ventral hippocampus and the lateral septum work in tandem to regulate rats' open-arm exploration in the elevated plus-maze. *Physiol Behav* 2010;101:141-152.

64. Anthony TE, Dee N, Bernard A, Lerchner W, Heintz N, Anderson DJ. Control of stress-induced persistent anxiety by an extra-amygdala septohypothalamic circuit. *Cell* 2014;156:522-536.
65. Nieh EH, Kim SY, Namburi P, Tye KM. Optogenetic dissection of neural circuits underlying emotional valence and motivated behaviors. *Brain Res* 2013;1511:73-92.
66. Jennings JH, Sparta DR, Stamatakis AM, et al. Distinct extended amygdala circuits for divergent motivational states. *Nature* 2013;496:224-228.
67. Li Y, Zhong W, Wang D, et al. Serotonin neurons in the dorsal raphe nucleus encode reward signals. *Nat Commun* 2016;7:10503.
68. Bang SJ, Commons KG. Forebrain GABAergic projections from the dorsal raphe nucleus identified by using GAD67-GFP knock-in mice. *J Comp Neurol* 2012;520:4157-4167.
69. Varga V, Losonczy A, Zemelman BV, et al. Fast synaptic subcortical control of hippocampal circuits. *Science* 2009;326:449-453.
70. Mead GE, Hsieh CF, Lee R, et al. Selective serotonin reuptake inhibitors for stroke recovery: a systematic review and meta-analysis. *Stroke* 2013;44:844-850.